

UCLA

UCLA Previously Published Works

Title

Coupled Climate-Economic Modes in the Sahel's Interannual Variability

Permalink

<https://escholarship.org/uc/item/96w1d1rs>

Journal

Ecological Economics, 153(C)

ISSN

0921-8009

Authors

Garnot, Vivien Sainte Fare

Groth, Andreas

Ghil, Michael

Publication Date

2018-11-01

DOI

10.1016/j.ecolecon.2018.07.006

Peer reviewed

1 Coupled climate-economic modes in the Sahel’s
2 interannual variability

3 Vivien Sainte Fare Garnot^{a,*}, Andreas Groth^b, Michael Ghil^{a,b}

4 ^a*Geosciences Department and Laboratoire de Météorologie Dynamique (CNRS and IPSL),
5 Ecole Normale Supérieure and PSL Research University, 24, rue Lhomond, 75005 Paris,
6 France*

7 ^b*Department of Atmospheric and Oceanic Sciences, University of California at Los
8 Angeles, Los Angeles, California, USA*

9 **Abstract**

 We study the influence of interannual climate variability on the economy
of several countries in the Sahel region. In the agricultural sector, we are able
to identify coupled climate-economic modes that are statistically significant on
interannual time scales. In particular, precipitation is a key climatic factor for
agriculture in this semi-arid region. Locality and diversity characterize the Sa-
hel’s climatic and economic system, with the coupled climate-economic patterns
exhibiting substantial differences from country to country. Large-scale atmo-
spheric patterns — like the El Niño–Southern Oscillation and its quasi-biennial
and quasi-quadrennial oscillatory modes — have quite limited influence on the
economies, while more location-specific rainfall patterns play an important role.

10 *Keywords:* Advanced spectral methods, Business cycles, Climate cycles,
11 Climate impacts on the economy, Sahel climate

12 **1. Introduction**

13 The study of climate impacts on the economy is a crucial part of assessing
14 the stakes of ongoing global climate change. Thus, [Stern \(2016\)](#) called climate
15 scientists for a closer collaboration with economists to design better models and
16 impact assessment methods. This endeavor, though, requires one to better un-
17 derstand the interactions between two complex chaotic systems: the climatic

*Corresponding author
Preprint submitted to *Environmetrics* on August 17, 2018
Email address: vivien.steinfaregarnot@polytechnique.edu (Vivien Sainte Fare Garnot)

18 and the economic one. To cope with this problem, common approaches circum-
19 vent the very difficult task of describing the internal dynamics of either system,
20 as well as the nonlinear interactions between the two. Typically, they do so
21 either by formulating damage functions that have little empirical basis or by
22 applying crude regressions to historical time series.

23 The present work explores an alternative way based on advanced spectral
24 decomposition methods. We focus here on the identification of endogenous
25 dynamics in both the climatic and economic system, and the detection of coupled
26 climate-economic behavior on interannual time scales.

27 To identify patterns of spatio-temporal behavior in complex datasets, we rely
28 on multichannel singular spectrum analysis (M-SSA), which provides an efficient
29 tool to detect and reconstruct oscillatory modes from short and noisy time
30 series; see [Ghil et al. \(2002\)](#) and [Alessio \(2016, chapter 12\)](#) for a comprehensive
31 overview of the methodology and of related spectral methods.

32 M-SSA is based on classical [Karhunen \(1946\)](#)-[Loève \(1945\)](#) theory and was
33 introduced into the analysis of nonlinear dynamical systems by [Broomhead and](#)
34 [King \(1986a,b\)](#). The methodology has found since countless applications in the
35 geosciences (e.g., [Vautard and Ghil, 1989](#); [Ghil and Vautard, 1991](#)) and beyond.
36 More recently, M-SSA has been applied to study the dynamics of macroeconomic
37 activity in the US ([Groth et al., 2015](#)) and the synchronization of business cycles,
38 first in a set of three European countries ([Sella et al., 2016](#)) and then in more
39 than 100 countries around the world ([Groth and Ghil, 2017](#)).

40 We combine here the climatic and economic system in a cross-panel M-SSA
41 analysis to study coupled climate-economic behavior in the Sahel region. It turns
42 out that, in this setting, M-SSA greatly helps identifying signals of interannual
43 climate variability in the economic time series.

44 The Sahel's climate is very erratic and repeatedly suffered from severe droughts
45 ([Nicholson, 2013](#)); it remains unclear whether the series of droughts has stopped
46 now or not ([Masih et al., 2014](#)). Precipitation variability is a key climatic factor
47 for agriculture in semi-arid regions, and thus climate change entails increased
48 risk in such regions ([Dilley, 1997](#)). This issue, combined with the high demo-

49 graphic and economic stress on the region, makes it highly vulnerable and hence
50 even more critical to investigate.

51 Thus, in addition to confirming the cyclic nature of climate and the economy,
52 the paper's aim is to *determine whether climatic oscillations manifest themselves*
53 *in macro-economic time series from the Sahel region*. To achieve this aim, we
54 apply M-SSA to a dataset aggregating economic and climatic time series from
55 the region. To the best of our knowledge, such an approach has not been tried
56 yet in the ecological economics literature, and the present paper should be read
57 as a proof of concept.

58 The paper is organized as follows. In Sec. 2, we give a brief introduction
59 to the M-SSA methodology and present a novel statistical significance test that
60 is tailored to this paper's specific problems. Details about the dataset and the
61 framework of the study are given in Sec. 3, while general characteristics of the
62 time series are briefly presented in Sec. 4. In Sec. 5, we discuss the spectral
63 properties of the combined, climatic-and-economic dataset, while coupled
64 climate-economic behavior is analyzed in Sec. 6. The results are discussed in
65 Sec. 7, and the paper concludes with a summary in Sec. 8.

66 **2. Methodology**

67 In Sec. 2.1, we briefly describe the main steps of the M-SSA methodology,
68 while in Sec. 2.2, the methodology for statistical-significance testing is intro-
69 duced.

70 *2.1. M-SSA*

71 The main aspects of M-SSA are summarized here, and the reader can refer
72 to Ghil et al. (2002) and Alessio (2016, chapter 12) for further details. A helpful
73 illustration of the main mathematical aspects can be found in Groth and Ghil
74 (2017).

75 The algorithm involves four main steps: (1) embedding, (2) decomposition,
76 (3) rotation, and (4) reconstruction; these steps are outlined in the following.

Embedding. Consider a multivariate time series $\{x_d(n) : n = 1 \dots N; d = 1 \dots D\}$, with D channels of length N ; the first step of M-SSA is to embed each channel into an M -dimensional space, where M , the window length, is a parameter. The *trajectory matrix* is thus generated by taking successive M -lagged copies from the original series:

$$\mathbf{X}_d = \begin{pmatrix} x_d(1) & x_d(2) & \cdots & x_d(M) \\ x_d(2) & x_d(3) & \cdots & x_d(M+1) \\ \vdots & & & \vdots \\ x_d(N-M+1) & \cdots & & x_d(N) \end{pmatrix} \quad (1)$$

Hence each trajectory matrix \mathbf{X}_d is composed of M columns of reduced length $N' = N - M + 1$. The *augmented trajectory matrix* is then formed by concatenating all D channels,

$$\mathbf{X} = [\mathbf{X}_1, \mathbf{X}_2, \dots, \mathbf{X}_D]. \quad (2)$$

77 *Decomposition.* M-SSA then proceeds by performing a Singular Value Decom-
78 position (SVD) of the augmented trajectory matrix,

$$\mathbf{X} = \eta^{1/2} \mathbf{P} \mathbf{\Sigma} \mathbf{E}', \quad (3)$$

79 where $(\cdot)'$ denotes the transpose of the argument and the normalization factor
80 η equals $\max\{N', DM\}$. The decomposition yields a set of κ non-vanishing sin-
81 gular values $\{s_1, \dots, s_\kappa\}$, arranged in descending order along the main diagonal
82 of matrix $\mathbf{\Sigma}$, with $\kappa = \min\{N', DM\}$ being the rank of \mathbf{X} . The matrix \mathbf{P} of
83 left-singular vectors has size $N' \times \kappa$ and provides a set of κ temporal EOFs (T-
84 EOFs). These T-EOFs of reduced length N' reflect the corresponding behavior
85 of an oscillation.

The matrix \mathbf{E} of right-singular vectors has size $DM \times \kappa$ and provides a set of space-time empirical orthogonal functions (ST-EOFs), arranged as κ columns of length DM ; it is composed of D consecutive segments \mathbf{E}_d of size $M \times \kappa$,

$$\mathbf{E}' = [\mathbf{E}'_1, \mathbf{E}'_2 \dots \mathbf{E}'_D], \quad (4)$$

each of which is associated with a channel \mathbf{X}_d in \mathbf{X} .

Combining Eqs. (2)–(4), we can easily reformulate Eq. (3) into a channel-wise notation,

$$\mathbf{X}_d = \eta^{1/2} \mathbf{P} \boldsymbol{\Sigma} \mathbf{E}'_d. \quad (5)$$

A helpful discussion and illustration of these mathematical properties can be found in Groth and Ghil (2017, Sec. III and Fig. 1).

Rotation. To better separate distinct oscillations, we rely here on a modified varimax rotation of the ST-EOFs, cf. Groth and Ghil (2011) and Portes and Aguirre (2016).

Reconstruction. The dynamical behavior of \mathbf{X} associated with a subset $\mathcal{K} \subseteq \{1, \dots, \kappa\}$ of ST-EOFs can be obtained from Eq. (3) by

$$\mathbf{R}_{\mathcal{K}} = \eta^{1/2} \mathbf{P} \boldsymbol{\Sigma} \mathbf{K} \mathbf{E}'; \quad (6)$$

here \mathbf{K} is a diagonal matrix of size $\kappa \times \kappa$, with the k -th diagonal element equal to one if $k \in \mathcal{K}$ and zero otherwise. Averaging along the skew diagonals of $\mathbf{R}_{\mathcal{K}}$, i.e., over elements that correspond in Eq. (1) to the same instant in time, finally yields the reconstructed components (RCs).

Participation index. The squares s_k^2 of the singular values equal the eigenvalue λ_k and quantify the variance in \mathbf{X} that is captured by the corresponding EOF, i.e. the k -th column in \mathbf{E} . The contribution of channel d to this variance can be measured by the *participation index*,

$$\pi_{dk} = s_k^2 \sum_{m=1}^M e_{dk}^2(m), \quad (7)$$

where the sum ranges over all the elements of the k -th column in \mathbf{E}_d . Since the singular vectors have norm one, we get

$$\sum_{d=1}^D \pi_{dk} = s_k^2, \quad (8)$$

i.e. the sum of all D participation indices for a given EOF k yields the corresponding variance λ_k (Groth and Ghil, 2011).

98 *Remark.* We have followed here the original trajectory-matrix approach of [Broom-](#)
 99 [head and King \(1986a,b\)](#), which relies on an SVD of \mathbf{X} in Eq. (3). Alterna-
 100 tively, one could obtain \mathbf{E} from the eigendecomposition of the covariance matrix
 101 $\eta^{-1}\mathbf{X}'\mathbf{X} = \mathbf{E}\mathbf{\Lambda}\mathbf{E}'$ ([Vautard and Ghil, 1989](#)), with the eigenvalues $\mathbf{\Lambda} = \mathbf{\Sigma}^2$. How-
 102 ever, in the case of a rank-deficient covariance matrix, i.e. $DM > N'$, it is
 103 more efficient to calculate the eigendecomposition from a reduced covariance
 104 matrix, $\eta^{-1}\mathbf{X}\mathbf{X}' = \mathbf{P}\mathbf{A}\mathbf{P}'$ ([Allen and Robertson, 1996](#)). Irrespective of the chosen
 105 algorithm, all approaches yield the same nonvanishing eigenelements ([Groth](#)
 106 [and Ghil, 2015](#)), and we use the two terms, singular values and eigenvalues,
 107 interchangeably here.

108 *Oscillatory modes.* M-SSA provides a decomposition of the dataset into distinct
 109 spectral components. The EOFs, though not purely sinusoidal, tend to have a
 110 dominant frequency that can be determined via their Fourier transform ([Vau-](#)
 111 [tard and Ghil, 1989](#)). It is, therefore, common practice to plot the eigenvalues
 112 against their corresponding dominant frequencies to obtain an estimate of a time
 113 series' spectral decomposition; as initially suggested by [Allen and Smith \(1996\)](#),
 114 doing so is more informative than the still widespread practice of providing the
 115 “scree diagram” of eigenvalues against their rank.

116 Like the sine-cosine pairs in a Fourier analysis, the EOFs tend to pair up into
 117 oscillatory pairs ([Vautard and Ghil, 1989](#)). The two EOFs in such a pair are
 118 in phase quadrature and they capture the symmetric and antisymmetric parts
 119 of the oscillation: hence, they also have nearly equal dominant frequencies and
 120 variance levels.

121 The varimax rotation introduced by [Groth and Ghil \(2011\)](#) greatly improves
 122 the pairing of EOFs and the separation between EOFs associated with distinct
 123 dominant frequencies. In the absence of rotation, M-SSA is subject to a de-
 124 generacy problem and can generate spurious coupled oscillations ([Feliks et al.,](#)
 125 [2013](#)). A careful varimax-rotated M-SSA analysis will be used here in the search
 126 for coupled oscillatory modes in the climatic and economic series.

127 Still, EOF pairing, while necessary, is not a sufficient criterion to determine

128 whether or not an oscillatory component is present in the time series. The infor-
129 mal ranking of the eigenvalues in descending order of captured variance should
130 not be confused with the order of significance. It is only by testing against
131 a specific null hypothesis that further conclusions about significant oscillations
132 can be drawn. Several methods have been proposed to test the statistical sig-
133 nificance of oscillations, and the most solidly established one as yet is Monte
134 Carlo SSA.

135 *2.2. Significance test*

136 *Monte Carlo SSA (MC-SSA)*. The idea of MC-SSA is to test the statistical
137 significance of the variance level of each eigenvalue using a Monte Carlo-type
138 technique. The algorithm starts by fitting an autoregressive (AR) process of
139 order 1 to each input channel of the dataset. The parameters are chosen such
140 that this process has the same lag-0 and lag-1 covariance as the time series.
141 An ensemble of surrogate realizations for the time series is next generated from
142 the AR(1) process, which is then projected onto the data EOFs to derive a
143 null-hypothesis distribution of variance levels for the significance test of the
144 eigenvalues.

145 For a more complete exposition of MC-SSA see [Allen and Smith \(1996\)](#)
146 and [Allen and Robertson \(1996\)](#), while [Groth and Ghil \(2015\)](#) provide a recent
147 review of different MC-SSA techniques. A detailed application to the study of
148 economic cycles can be found in [Groth et al. \(2015\)](#).

149 *Significance test of participation index*. In the original formulation of the single-
150 channel MC-SSA significance test, the eigenvalue of a given EOF is tested
151 against the null hypothesis of a single AR(1) process ([Allen and Smith, 1996](#)).
152 In the multichannel case, though, a principal component analysis (PCA) is per-
153 formed on the dataset prior to M-SSA, and MC-SSA is then carried out on the
154 principal components (PCs), cf. [Allen and Robertson \(1996\)](#). The latter step
155 is intended to avoid any weakening of the test against the null hypothesis of D
156 independent AR(1) processes, due to correlations in the dataset.

157 The prior PCA analysis does not hinder the study of the spectral properties
 158 of the dataset, i.e. the M-SSA eigenvalues are invariant with respect to the
 159 PCA, yet the results are more abstract and harder to interpret in the PC space.
 160 The multichannel MC-SSA test will only assess whether the variance λ_k for a
 161 given EOF captured in all channels together is statistically significant.

162 In the present context, though, where mixed datasets of economic and cli-
 163 matic time series are analyzed, a modification is required as we wish to assess
 164 whether the variance of any of these channels is individually significant. A novel
 165 version of the MC-SSA methodology is therefore presented here that allows us
 166 to test the significance of the participation index π_{dk} instead.

167 Without any prior PCA, the algorithm starts to fit independent AR(1) pro-
 168 cesses to each of the D input channels. In the next step, an ensemble of surrogate
 169 realizations is generated, as in the standard MC-SSA test. For each surrogate
 170 realization, we form the channel-wise augmented trajectory matrix $\mathbf{X}_{R,d}$ for
 171 each input channel d as in Eq. (1) and, finally, the overall augmented trajectory
 172 matrix $\mathbf{X}_R = [\mathbf{X}_{R,1}, \dots, \mathbf{X}_{R,D}]$, following Eq. (2).

In the classical version, due to [Allen and Robertson \(1996\)](#), of a multichannel
 MC-SSA test, the next step is to project the reduced covariance matrix $\mathbf{X}_R \mathbf{X}'_R$
 onto the matrix of left-singular vectors \mathbf{P} ,

$$\mathbf{\Lambda}_R = \eta^{-1} \mathbf{P}' \mathbf{X}_R \mathbf{X}'_R \mathbf{P}, \quad (9)$$

173 to derive the significance level for the eigenvalues, $\mathbf{\Lambda} = \eta^{-1} \mathbf{P}' \mathbf{X} \mathbf{X}' \mathbf{P}$, from the
 174 statistics of the diagonal elements of $\mathbf{\Lambda}_R$. In the terminology of [Groth and](#)
 175 [Ghil \(2015\)](#), this technique is referred to as unscaled target rotation onto the
 176 temporal EOFs (T-EOFs).

To understand the modifications of the significance test for the participation
 index, we remember that, following Eq. (2), the reduced covariance matrix of the
 multichannel dataset $\mathbf{X} \mathbf{X}'$ is simply the sum of D univariate covariance matrices
 $\mathbf{X}_d \mathbf{X}'_d$,

$$\mathbf{X} \mathbf{X}' = \sum_{d=1}^D \mathbf{X}_d \mathbf{X}'_d. \quad (10)$$

Note that, projecting the univariate covariance matrices onto \mathbf{P} and substituting $\mathbf{X}'_d\mathbf{P} = \eta^{-1/2}\mathbf{E}_d\mathbf{\Sigma}$ according to Eq. (5), we obtain

$$\eta^{-1}\mathbf{P}'\mathbf{X}_d\mathbf{X}'_d\mathbf{P} = \mathbf{\Sigma}'_d\mathbf{E}_d\mathbf{\Sigma} = \mathbf{\Pi}_d, \quad (11)$$

177 a diagonal matrix $\mathbf{\Pi}_d$ of size $\kappa \times \kappa$ with the k -th diagonal element equal to π_{dk} .
178 The latter follows from the definition of π_{dk} in Eq. (7).

The modified significance test therefore proceeds, by analogy with Eq. (9), by projecting the univariate covariance matrices of the surrogate realizations onto \mathbf{P} ,

$$\eta^{-1}\mathbf{P}'\mathbf{X}_{R,d}\mathbf{X}'_{R,d}\mathbf{P} = \mathbf{\Pi}_{R,d}, \quad (12)$$

179 to derive the significance level for the participation indices $\mathbf{\Pi}_d$ from the statistics
180 of the diagonal elements of $\mathbf{\Pi}_{R,d}$.

181 Recall that this test on a common oscillatory mode differs from that of mul-
182 tiple univariate MC-SSA tests, in which the different EOF solutions are initially
183 not linked. The observation of EOFs with similar dominant frequencies in dif-
184 ferent input channels, though, is only a necessary but not sufficient condition for
185 the presence of coupled oscillations. It is the refined varimax M-SSA solution
186 with the novel MC test presented herein that allows a more detailed analysis of
187 shared mechanisms and of each channel's individual contribution to it.

188 Moreover, if we wish to exclude a certain part of the time series from the
189 significance test, such as the dominant trend, we follow the approach of an M-
190 SSA composite null hypothesis (Groth and Ghil, 2015). The essential idea is to
191 fit an AR(1) process to the RCs, as defined in Eq. (6), in which the diagonal
192 elements of \mathbf{K} equal 1 if we wish to test the corresponding EOFs and 0 otherwise.
193 In the same way, dominant oscillatory modes that are found significant in a first
194 run of the significance test can likewise be excluded from a second run of the
195 test; see Allen and Smith (1996) for further details on this iterative process.

196 It is important to point out that, in contrast to the common idea of first
197 detrending the dataset prior to any spectral analysis, our single-step M-SSA
198 analysis with its composite technique is not subject to the problem of spurious
199 oscillations due merely to the detrending procedure itself (Nelson and Kang,

200 [1981](#); [Harvey and Jaeger, 1993](#); [Cogley and Nason, 1995](#)). Instead, our single-
201 step M-SSA analysis provides us with a more consistent separation into a per-
202 manent trend component and transitory fluctuations that are orthogonal to it
203 ([Groth and Ghil, 2017](#)).

204 **3. Experimental setting**

205 *Time boundaries.* In the choice of the time interval for the analysis, the limiting
206 factor is the availability of the economic data: while climate data are available
207 for the whole 20th century, the economic dataset chosen here is only available
208 starting in 1960. Therefore, the time interval analyzed herein extends from 1960
209 to 2015. Though quite limited, this interval does have a satisfactory length for
210 the spectral analysis of interannual variability.

211 The sampling interval chosen for the present study is one sample per year,
212 which suffices to resolve periodicities of 2 years and longer. The aggregated
213 economic series analyzed here are already provided in this form, and the climate
214 series, though available every month, were converted into yearly time series as
215 well. In doing so, the monthly series were first low-pass filtered with a Chebyshev
216 type I filter¹ to remove periodicities shorter than 2 years and then annually
217 sub-sampled by simply taking all July values; see [Feliks et al. \(2013\)](#) and the
218 appendix therein for additional details on the low-pass filtering.

219 *Space boundaries.* The Sahel represents a transitional zone, between the Sahara
220 desert to the North and the subtropical Savannah grasslands to the South, and
221 it thus has a semi-arid climate. When studied in a purely climatic context, the
222 Sahel is defined as the region in which the rainfall is generally limited to the
223 boreal summer months, with maximum rainfall occurring in August ([Nicholson,](#)
224 [2013](#)).

¹When its parameters are optimized, this filter exhibits practically no distortions of either phase or amplitude in the passband, and a highly effective damping in the stopband. We used the following filter parameters: cutoff frequency $1/2.16 \text{ year}^{-1}$, order 8, and ripple factor 0.001.

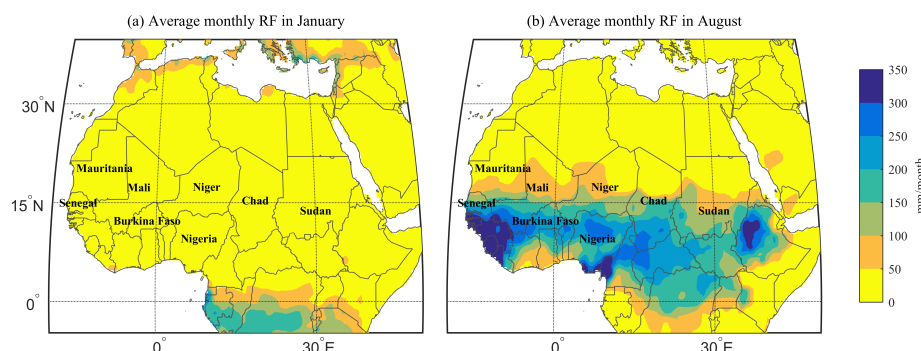


Figure 1: Average monthly rainfall in (a) January and (b) August. The average is calculated over the interval 1942–2012 from the National Oceanic and Atmospheric Administration (NOAA) PRECipitation REConstruction over Land (PREC/L) dataset (Chen et al., 2002), as given at www.esrl.noaa.gov/psd.

225 Figure 1 shows the average rainfall level in the region in January and August,
 226 corresponding to the dry and rainy season, respectively. Following Nicholson
 227 (2013), the Sahel covers the region between the latitudes of roughly 14°N and
 228 18°N , and ranges from Sudan in the East to Senegal in the West. It includes the
 229 countries of Burkina Faso, Chad, Mali, Mauritania, Niger, Nigeria, Senegal, and
 230 Sudan². The two countries Mali and Nigeria were excluded from the present
 231 study, due to a significant part of the economic data missing for the two.

232 *Datasets.* Four indicators were chosen to reflect the evolution of the economic
 233 and climatic systems of the Sahel. The gross domestic product (GDP) and
 234 agriculture value added (AVA) for the economy, and the temperature (T) and
 235 rainfall (RF) for climate. The GDP was chosen as a common aggregated mea-
 236 surement of economic activity, while AVA was added to study these countries'
 237 economies strong dependence on their agricultural sector. Furthermore, as agri-
 238 culture in the Sahel is still mostly rainfed with little development of irrigation
 239 techniques, cf. (Rockström et al., 2009, Fig. 2.3), one can expect to see climate
 240 effects more directly in AVA than in GDP.

²Sudan here denotes both the recently separated countries of Sudan and South Sudan.

241 The two economic indicators were taken from the World Development In-
242 dicators Database³ and the two climate indicators from the Climate Change
243 Knowledge Portal⁴. The GDP and AVA series are both expressed in constant
244 2010 US\$. While the dataset for GDP was complete, missing AVA values were
245 estimated by taking AVA in current US\$ and dividing it by the GDP defla-
246 tor. For Mali and Nigeria, however, AVA values are missing in both constant
247 and current US\$; hence, we have excluded these two countries from the present
248 study.

249 Prior to M-SSA, the different indicators were all centered and normalized
250 to have unit variance. Note that no prior detrending of the time series was
251 performed to avoid problems of spurious oscillations, as already discussed in
252 Sec. 2.2.

253

254 4. General characteristics

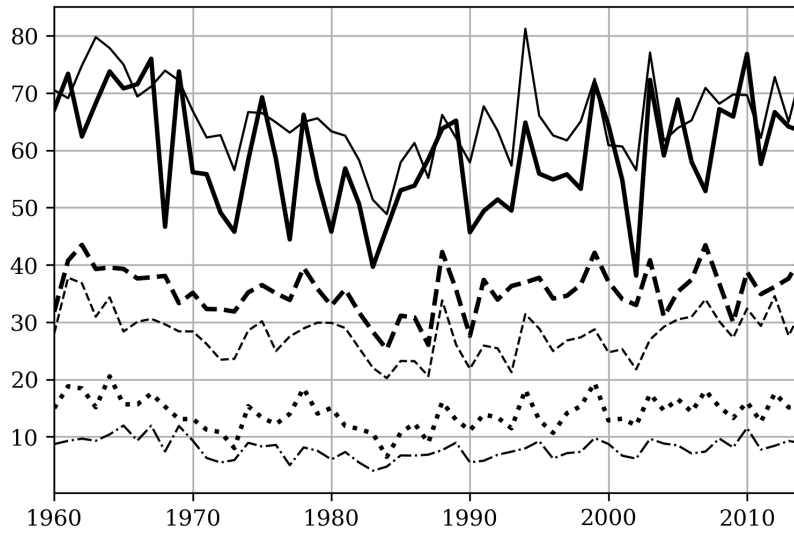
255 4.1. Climatic indicators

256 The climate time series are shown in Fig. 2. In the Sahel, though, rain falls
257 during only a few summer months, so that the August peak value in Fig. 1(b),
258 given in mm/month, is much higher than the annual value in Fig. 2(a), given in
259 mm/year. A simple linear regression between the annual values and the peak
260 values shows that the latter are roughly 4–6 times larger, depending on the
261 length of the rainy season in these countries.

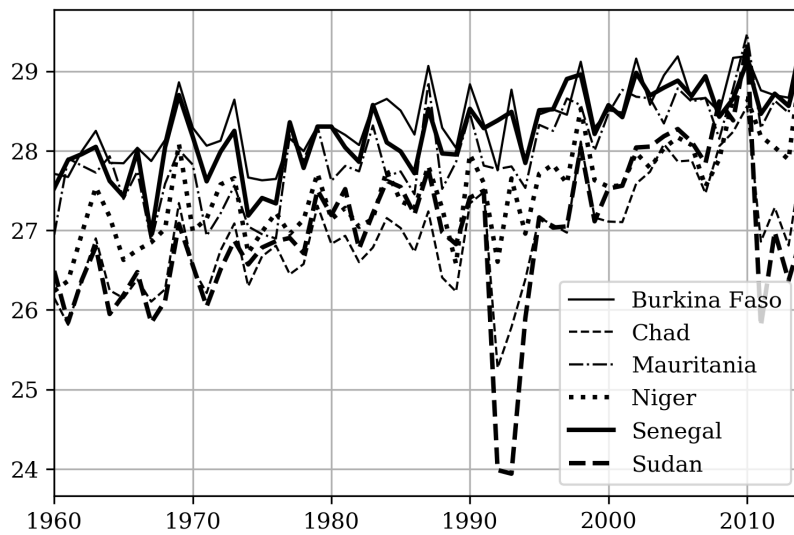
262 In the rainfall time series in Fig. 2(a), a pronounced downward trend is
263 apparent, especially for the high rainfall rates in Burkina Faso and Senegal,
264 from 1960 to the mid-1980s. This downward trend correlates well with the
265 decrease in the overall Sahel precipitation index for the area (20–10°N, 20°W–
266 10°E) (Janowiak, 1988; Becker et al., 2013), as archived at the Joint Institute

³data.worldbank.org/data-catalog/world-development-indicators

⁴sdwebx.worldbank.org/climateportal



(a) Rainfall (mm/year)



(b) Temperature (°C)

Figure 2: Climate time series of the six Sahel countries analyzed herein; see text in Sec. 3 for details of the annual sub-sampling of the monthly raw time series used here to get the plotted data.

267 for the Study of the Atmosphere and Ocean⁵. A milder increase in this index,
268 and in the country-wise rainfall rates in our Fig. 2(a), follows from that point
269 on to 2015.

270 High-amplitude year-to-year variability is superimposed on these trends, and
271 accounts for the intense, occasionally multiannual droughts that have occurred
272 most recently in 2010 and 2012. The droughts do not appear clearly, though, in
273 the temperature time series that are plotted in Fig. 2(b), which mainly shows a
274 warming trend of around 1°C over the whole time interval.

275 While the Sahel is often treated as one entity in the climate context, [Nichol-](#)
276 [son \(2013\)](#) already pointed out that notable contrasts across the region do exist.
277 This complexity is also reflected in Fig. 2, in which the rainfall and temperature
278 levels do show common traits but also substantial differences.

279 As a consequence of the strong seasonality in the rainbelt position, we ob-
280 serve roughly three types of rainfall profiles in Fig. 2(a), as one crosses the Sahel
281 from North to South:

- 282 • *Low rainfall exposure*: Countries furthest north, with only little of their
283 territory exposed to a low level of rainfall during the rainy season. Mauri-
284 tania and Niger fall into this category and have the lowest rainfall levels.
- 285 • *Intermediate rainfall exposure*: Countries extending further south, such
286 as Chad and Sudan, with around half of their territory exposed to in-
287 termediate rainfall during the rainy season, have higher overall rainfall
288 levels.
- 289 • *High rainfall exposure*: Countries with a significant part of their territory
290 exposed to high intensity rainfall during the rainy season. Of the six
291 countries considered here, Burkina Faso and Senegal fall into this category
292 and have therefore the highest annual rainfall levels. Still, the rainfall in
293 Senegal is more variable from year to year than in Burkina Faso. This
294 difference is mainly due to Senegal's being closer to the northern limit

⁵[doi:10.6069/H5MW2F2Q](https://doi.org/10.6069/H5MW2F2Q)

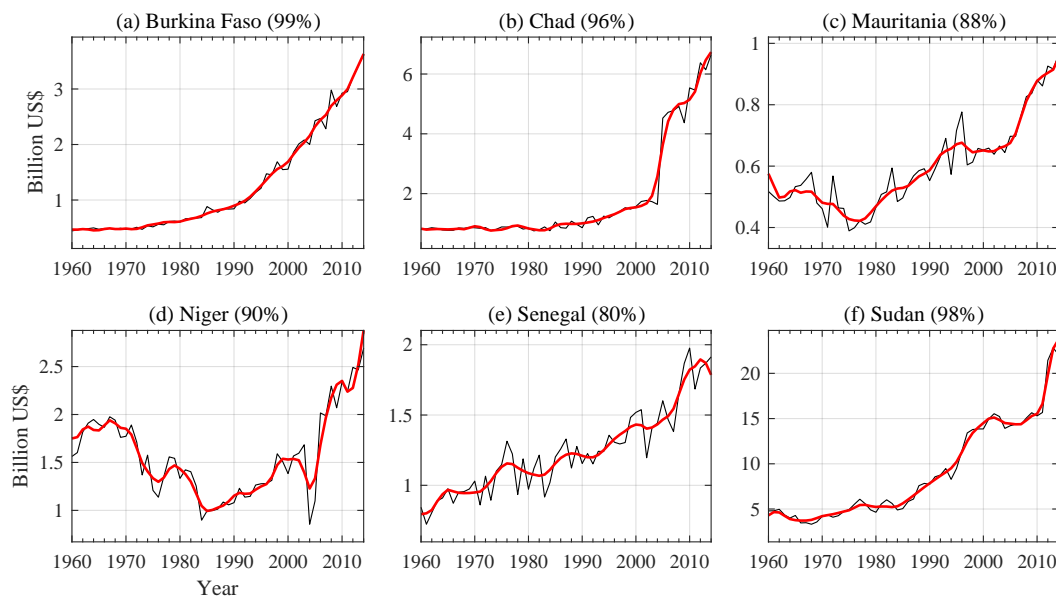


Figure 3: AVA time series (black) and estimated trend component (bold red). The trend for each country is estimated from low-frequency RCs with periods longer than 10 years, cf. Fig. 4 for additional details. The variance it captures in the AVA of each country is given in the legend of the corresponding panel (in %). Note the different scales on the y -axis.

295 of the rainbelt, whereas Burkina Faso is closer to the core. The latter is
 296 therefore less exposed to small year-to-year shifts in the rainbelt position.

297 4.2. Economic indicators

298 All six countries follow a pattern of a more or less persistent growth in GDP,
 299 with very little year-to-year variations and only a minor drop associated with
 300 the big recession of 2008 (not shown).

301 This GDP behavior is totally different from what we observe in the six AVA
 302 time series, shown in Fig. 3. Although persistently increasing in most of the
 303 countries, AVA is much less regular and subject to substantial variability overall,
 304 with behavior that also differs quite strikingly from country to country. Some
 305 countries, like Burkina Faso and Chad, have a more persistent trend and little
 306 year-to-year variation, while others — like Mauritania, Niger, and Senegal —
 307 have both an erratic trend and intense year-to-year fluctuations.

Table 1: Share of AVA in GDP (in %)

Country	1960	2015
Burkina Faso	38	32
Chad	40	51
Mauritania	76	18
Niger	75	37
Senegal	24	13
Sudan	51	32

308 Generally speaking, the trend residuals of AVA capture up to 20% of the
309 variance, while in GDP the residual variance does not exceed 2% (not shown).
310 This pronounced variability is consistent with the lack of agricultural technolo-
311 gies such as irrigation in the Sahel, insofar as such technologies would tend to
312 stabilize agricultural production (Rockström et al., 2009). Moreover, the strong
313 year-to-year variability in AVA raises the question of potential links to climate
314 variability on interannual time scales.

315 Table 1 lists the share of AVA in GDP for each of the six countries, in 1960
316 and 2015, respectively. In 1960, almost all economies were strongly dependent
317 on the agricultural sector, which accounts for more than a third of GDP in the
318 six countries, except for Senegal. In 2015, the dependency is still quite strong
319 for most of the countries, while only Senegal and Mauritania seem to be on the
320 way to a more industrialized economy.

321 5. Spectral characteristics

322 We start in this section by applying M-SSA to identify oscillatory behavior
323 in each of the two systems, climatic and economic, separately.

324 5.1. Economic indicators

325 A first set of tests was carried out on each of the two economic indicators,
326 GDP and AVA, separately. For each of the two indicators, the six countries were

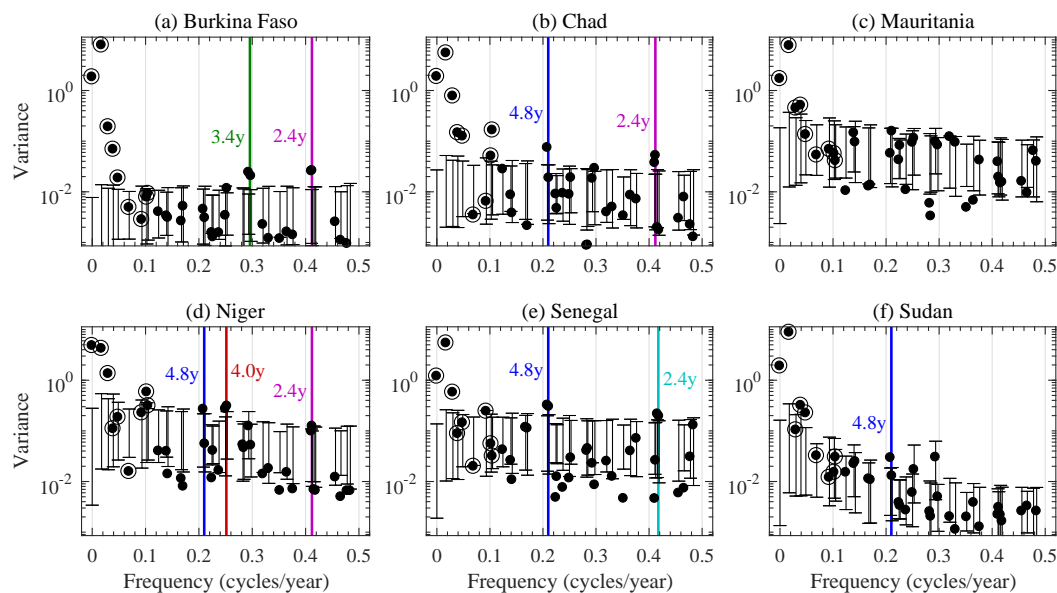


Figure 4: Cross-country M-SSA analysis of the six AVA time series from Fig. 3. Significant oscillatory modes are indicated by solid vertical lines; the colors identify distinct modes (see text for details). The M-SSA analysis here uses a window length of $M = 18$ years; the subsequent varimax rotation uses ST-EOFs 3–40. (a–f) For each country, the participation index π in each mode is shown as filled black circles, plotted as a function of the corresponding dominant frequency. Lower and upper ticks on the error bars correspond to the 2.5% and 97.5% quantiles from a Monte Carlo test of the participation index π ; the test ensembles have 2500 members. In the composite null hypothesis, the low-frequency EOFs (target dots) with a period longer than 10 years are excluded from the test and the remaining EOFs are tested against AR(1) noise.

327 combined in a single M-SSA analysis to identify cross-country relationships in
 328 the Sahel region.

329 The M-SSA analysis of the six AVA time series in Fig. 4 shows a rather
 330 diverse picture of distinct significant modes in each of the countries. Such
 331 diversity in the M-SSA spectra is consistent with the strong diversity already
 332 seen in the time series of Fig. 3. The diversity of spectral characteristics apparent
 333 in Fig. 4 clearly indicates that the Sahel cannot really be considered as a single
 334 economic entity. Still, a number of significant oscillatory modes, such as the

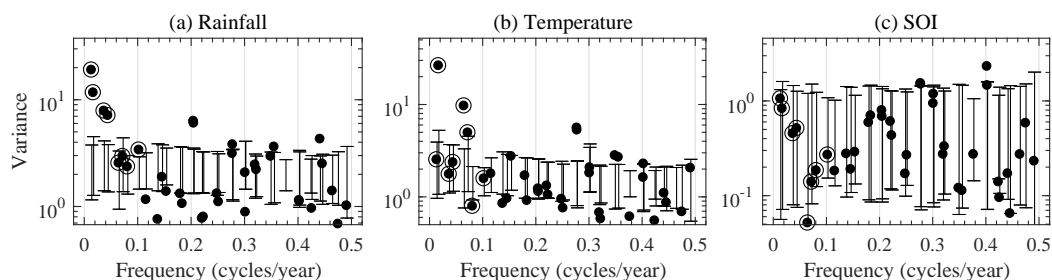


Figure 5: Cross-country M-SSA analysis of the six rainfall and six temperature time series in Fig. 2, and of the SOI index. In each mode, we plot the sum π of the of variances for (a) the six rainfall time series, and (b) the six temperature time series is shown; the significance levels are derived from a Monte Carlo test against the sum of surrogate participation indices. (c) Corresponding variance π of the SOI index. M-SSA and MC test parameters as in Fig. 4.

335 modes with a 4.8-year and 2.4-year periodicity, can be found in several countries.

336 A common oscillatory mode with a 2.4-year period is found in Burkina Faso,
 337 Chad and maybe Niger. Note that this common mode is distinct from a separate
 338 oscillatory mode of similar 2.4-year period in Senegal; i.e. M-SSA identifies the
 339 behavior in the latter mode to be uncoupled from the former one. Moreover,
 340 a common 4.8-year mode is found in Chad, Niger, Senegal, and Sudan. Other
 341 modes appear to be more country specific, with a 4-year mode in Niger and a
 342 3-year mode in Burkina Faso. In Mauritania, we are not able to identify any
 343 mode as statistically significant.

344 An equivalent M-SSA analysis was carried out on the six GDP time series
 345 (not shown), and it found similar but less numerous modes. Some of the modes
 346 we have identified in AVA are also present in the GDP spectra, a result that
 347 is consistent with the important role of the agriculture in the economy of these
 348 countries, cf. Table 1.

349 The variety of spectral patterns found here in the analysis of the economic
 350 indicators for the Sahel contrasts with the more synchronized behavior obtained
 351 when analyzing the economic series of developed countries within a given geo-
 352 graphic region, such as Europe, cf. Sella et al. (2016). This finding suggests a
 353 higher diversity in the spectral structure of the economies of developing coun-

354 tries within a given geographic region.

355 We have furthermore analyzed the possibility of coupled modes shared with
356 several major economies. To do so, we have added the GDP time series of the
357 US and France⁶ to our M-SSA analysis, but were not able to find any of the
358 above modes as being statistically significant in either of the two developed
359 countries, nor were we able to find additional coupled modes at other periods.

360 5.2. Climatic indicators

361 In the spectral analysis of the climatic indicators, we have chosen to combine
362 the rainfall and temperature time series of all six countries in a single M-SSA
363 analysis. To include effects of other large-scale phenomena such as the El Niño–
364 Southern Oscillation (ENSO) on the Sahel — which is known to influence the
365 West African monsoon (Janicot et al., 1996) we have furthermore chosen to
366 add the time series of the Southern Oscillation Index (SOI)⁷ to our M-SSA
367 analysis. The analysis presented here is only meant to give a brief idea of
368 interannual variability in this region; a comprehensive review can be found in
369 Nicholson (2013).

370 The M-SSA spectrum for the rainfall, temperature, and SOI time series is
371 plotted in Fig. 5. In this preliminary analysis of the climate indicators, we
372 provide only aggregated spectral properties for each of the indicators, while we
373 leave the detailed, country-specific analysis for Sec. 6. Figures 5(a) and 5(b)
374 thus provide only the sum of π over all rainfall and temperature time series,
375 respectively, in each of the modes.

376 Comparing the spectral properties of rainfall and temperature, we observe
377 quite a few distinct oscillations at periods similar to those in Fig. 4, while only
378 very few modes seem to be present in both temperature and rainfall dynamics.
379 In the spectrum of the SOI in Fig. 5(c), on the other hand, we are able to identify
380 two modes with periods of 3.6 years and 2.4 years, respectively. These two

⁶Note that four of the six countries under consideration are subject to France’s economic influence via the African Financial Community (CFA) zone.

⁷<http://www.bom.gov.au/climate/current/soihtm1.shtml>

381 modes agree well in their period lengths with the well-known quasi-quadrennial
382 and quasi-biennial oscillations present in many ENSO spectra (Rasmusson and
383 Carpenter, 1982; Jiang et al., 1995; Ghil et al., 2002), which seem therewith to
384 affect the Sahel’s rainfall and temperature fields.

385 6. Coupled climate-economy modes

386 Preliminary tests of a grand M-SSA, in which all four indicators of all six
387 countries were combined, gave only inconclusive results (not shown). Given
388 the diversity of spectral properties apparent in both the climate and the eco-
389 nomic datasets, this finding is not surprising, and this approach was, therefore,
390 discarded. A more specific, country-based analysis is adopted here instead.

391 After having confirmed the presence of oscillatory behavior in each indicator
392 individually in Sec. 5, we now evaluate connections between the climate and
393 economic indicators for each country separately. Country-based datasets were
394 formed with the four indicators concatenated in a single M-SSA analysis, and
395 applying the MC test procedure of Sec. 2.2 enables us to evaluate the statistical
396 significance of each indicator’s participation in coupled oscillatory modes.

397 The diversity of spectral characteristics that were found in each of the indi-
398 cators in Sec. 5 is also reflected here in the results of the country-based analysis,
399 and in the way the climate and economic system interact in each country. Table
400 2 summarizes the oscillatory modes that are significant in the country-based
401 analysis of Burkina Faso, Niger, Senegal, and Sudan. We focus on interannual
402 modes with periods of 2–10 years. The window length chosen here is $M = 18$
403 years and EOFs with periods longer than 10 years are considered to be part of
404 the long-term trend and excluded from the significance test. Whenever neces-
405 sary, other dominant oscillatory modes that were found significant in a first run
406 of the significance test, were likewise excluded from a second run of the test.
407 These modes are put into parentheses in Table 2. Note that the results for Chad
408 and Mauritania are not included in the table, since no highly significant coupled
409 modes were detected.

410 The majority of the modes are significant either in the climatic or in the
411 economic domain, but not in both. In temperature, for example, we see a
412 pervasive 3.6-year mode in all four countries. This mode was already detected in
413 Fig. 5(b) and it is likely to be linked to the quasi-quadrennial ENSO oscillation,
414 cf. Fig. 5(c); it is apparently not coupled, though, to any of the oscillatory
415 modes of the economic time series in Table 2.

416 A few purely economic modes are highly significant as well. In Table 2, we
417 see that Burkina Faso and Sudan both present oscillatory modes involving AVA
418 and GDP, which have periods of 3.3 and 4.0 years, respectively. The rigorous
419 application of the MC significance test shows that these modes are not merely
420 due to the detrending of random economic fluctuations and that endogenous,
421 deterministically generated variability has to be involved (Groth et al., 2015).

422 To which extent each of these endogenous modes can be attributed to ad-
423 justment delays and information lags in the market, as theorized by Kitchin
424 (1923), is beyond the scope of the present paper. Be that as it may, both peri-
425 ods are consistent with the 3–4-year period of Kitchin (1923) cycles, as reviewed
426 *in extenso* by Burns and Mitchell (1946). It appears, therefore, that some form
427 of excitation of endogenous business cycles by a quasi-periodic climatic forcing
428 might be at work in both countries.

429 Aside from the uncoupled modes in either the climatic or the economic sys-
430 tem, we are able to identify four coupled climate-economic modes with high
431 statistical significance, one in each country. These four are highlighted in bold
432 in Table 2. The agricultural sector is involved in all four modes, but no other
433 common feature can be found in all four. The details and specificities of each
434 country are discussed in the following subsections.

435 Before exploring these common modes further, it is interesting to dwell on
436 the lack thereof for two of the countries. In the case of Mauritania, this absence
437 is consistent with the absence of significant AVA modes in Fig. 4(c). Chad,
438 though, did exhibit two oscillatory AVA modes in Fig. 4(b); still, no evidence
439 of climate coupling could be found here.

440 In neighboring Sudan, on the other hand, we do observe a 4.8-year mode in

Table 2: Oscillatory modes found significant in country-based M-SSA analyses. Coupled climate-economic modes in bold. Oscillatory modes that were excluded from the composite null hypothesis appear in parentheses

Period (in years)	GDP	AVA	RF	T
Burkina Faso				
(4.8)			***	
3.6				***
3.3	**	***		
(2.8)			**	**
2.4	***	***	**	**
(2.2)			***	
Niger				
4.1		***	**	
3.6				***
(2.8)			***	**
(2.2)			**	
Senegal				
4.8		***	***	
3.6				***
3.0			**	
2.4		***		
2.3			**	
Sudan				
5.0	***	***		**
4.0	**	**		
(3.6)			***	**
3.0			**	
2.7			**	

*** at 99% and ** at 97.5% significance level; RF = rainfall; T = temperature.

441 AVA, cf. Fig. 4(f); this mode is similar to the one in Chad, yet only in Sudan
442 is a coupled oscillatory mode between AVA and temperature highly significant,
443 as indicated in bold in Table 2.

444 These country-to-country discrepancies can have various causes, including
445 the differences in their agricultural-vs.-industrial development, as per Table
446 1. The strong geographic diversity in the Sahel’s local terrain and vegetation
447 (Georganos et al., 2017) could also have played a role. However that may be, the
448 example of neighboring Chad vs. Sudan shows that the occurrence of coupled
449 climate-economic modes can be fairly localized. To which extent trade between
450 these two countries may have led to the presence of this 4.8-year mode in Chad’s
451 AVA has to be left for future studies.

452 6.1. Rainfall modes in Senegal and Niger

453 Niger and Senegal both present a coupled mode between rainfall and agricul-
454 ture, cf. Table 2, with a 4–5-year period. Figures 6(a,b) show the correspond-
455 ing spectral decompositions of AVA and rainfall, respectively, from the M-SSA
456 analysis of the four indicators for Senegal. The AVA spectrum in Fig. 6(a) is
457 consistent with the one we have already seen in the cross-country analysis of
458 AVA, as shown in Fig. 4(e). For Senegal, however, only the 4.8-year AVA mode
459 is significantly coupled with rainfall, while the country’s 2.4-year AVA mode is
460 not significantly coupled with a similar but distinct 2.4-year mode in rainfall.

461 The reconstruction of AVA and rainfall with the RCs of the 4.8-year mode is
462 shown in Figs. 6(c,d), respectively, together with the trend residuals; the latter
463 are obtained by subtracting the low-frequency trend components from the raw
464 data. In Senegal’s AVA, Fig. 6(c), the 4.8-year mode captures about one third
465 of the variance in the trend residuals and it provides a remarkably good fit to
466 its up-and-down swings.

467 In Senegal’s rainfall, Fig. 6(d), the 4.8-year mode captures about one quarter
468 of the variance and it still provides a remarkably good fit to the residuals.
469 Higher-frequency variations that correspond to the 2.4-year modes in AVA and
470 rainfall, respectively, become also apparent in the trend residuals. In AVA,

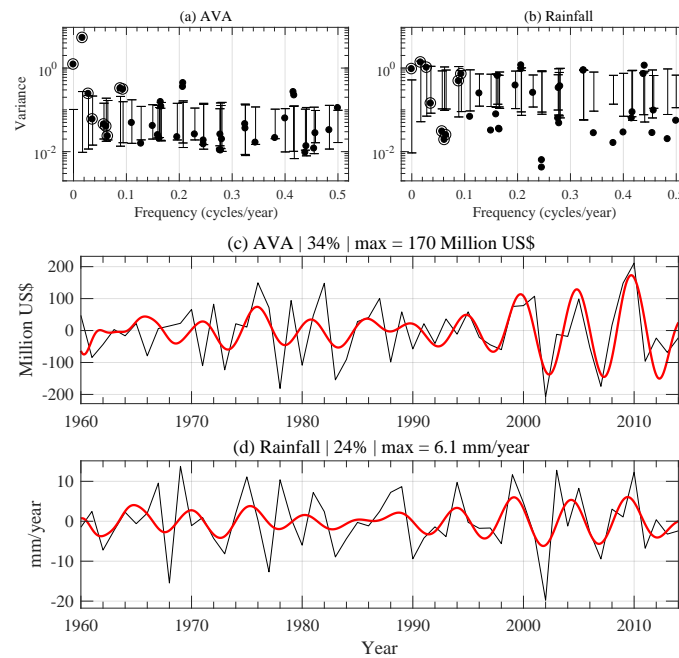


Figure 6: M-SSA analysis of the four indicators for Senegal. (a,b) Variance π of (a) AVA and (b) rainfall. (c, d) Reconstruction of the trend residuals (light black) with the RCs (heavy red) corresponding to the coupled 4.8-year mode in (c) AVA and (d) rainfall; the variance captured (in %) and the maximum values (max) are given in the legend. M-SSA and MC test parameters as in Fig. 4.

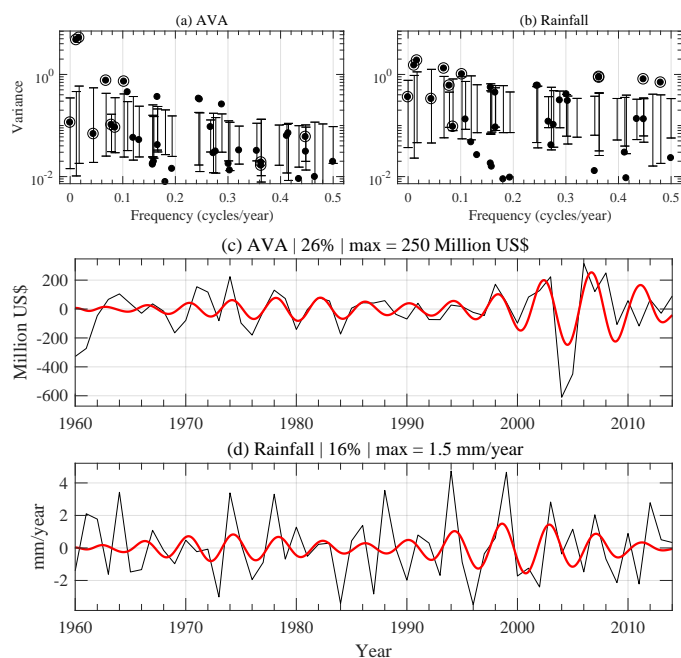


Figure 7: Same as Fig. 6, but for Niger. The reconstruction of the trend residuals (light black) in panels (c,d) uses here the RCs (heavy red) that correspond to the coupled 4.1-year mode in (c) AVA and (d) rainfall. M-SSA and MC test parameters as in Fig. 4, except two other EOF pairs, with a period of 2.8 years and 2.2 years, are excluded from the composite null hypothesis as well; see target dots in panel (a).

471 though, the 2.4-year mode is active during the first half of the interval only,
 472 while the 4.8-year mode begins to dominate after 1990. Although similar in
 473 their period length, M-SSA identifies the two 2.4-year modes in Figs. 6(a,b) as
 474 separate uncoupled modes, due to their different evolution in time (not shown).

475 The spectral decompositions of AVA and rainfall by the M-SSA analysis of
 476 the Niger dataset is shown in Figs. 7(a,b), respectively. In the composite test,
 477 we have furthermore excluded two pairs of EOFs with a period of 2.8 years and
 478 2.2 years; these two pairs correspond to pure climate oscillations, cf. Table 2. In
 479 doing so, it turns out that we are able to identify again a coupled mode in AVA
 480 and rainfall, although with a slightly different 4.1-year period. Recall that we
 481 found both a 4.8-year and a 4.1-year mode in Niger in the cross-country analysis

482 of AVA, as seen in Fig. 4(d); of these two, only the 4.1-year mode appears now
483 as a coupled climate-economic mode in Fig. 7(a).

484 The reconstruction of AVA and rainfall with the corresponding RCs is shown
485 in Figs. 7(c) and 7(d), respectively; the fit to the trend residuals is, once more, re-
486 markably good in periodicity and phase, but not in amplitude: indeed, Fig. 7(b)
487 shows that the 4.1-year mode captures only about 16% of the trend residuals'
488 variance in rainfall, due to the presence of other significant oscillatory modes.

489 In both countries, the RCs of AVA and rainfall clearly suggest direct effects
490 of rainfall variability on the AVA dynamics, while the amplitude ratio of the RCs
491 gives an estimate of the impact. For Senegal, an approximate 6 mm/year varia-
492 tion in rainfall corresponds to 170 million US\$ variations in AVA, cf. Figs. 6(c,d),
493 while for Niger, an approximate 1.5 mm/year variation in rainfall corresponds
494 to 250 million US\$ variations in AVA, cf. Figs. 7(c,d). This lower sensitivity
495 to rainfall variability in Senegal may result from differences in the exposure to
496 rainfall, as seen in Fig. 2(a). As already discussed in Sec. 4, Senegal benefits
497 from higher rainfall rates and it lies closer to the rainbelt core than Niger, so
498 that small year-to-year changes in rainfall levels are more critical for Niger.

499 6.2. *Temperature mode in Sudan*

500 In contrast to the two rainfall-related modes found in Senegal and in Niger,
501 Table 2 shows that our M-SSA analysis does not identify in Sudan a coupled
502 climate-economic mode involving rainfall. Instead, we find a 5.0-year tempera-
503 ture mode, coupled to both AVA and GDP; the corresponding RCs are shown in
504 Fig. 8. This 5.0-year mode provides a remarkably good fit to the trend residuals
505 of AVA in Fig. 8(b), as well as to the GDP ones in Fig. 8(a). The latter fit is
506 especially good after 1980, when the RCs reach their maximum amplitude.

507 Note that the RCs in temperature are anti-correlated with those of AVA and
508 GDP, i.e. an increase in temperature has a negative effect on the economy. The
509 amplitude ratio of the RCs suggests that an increase of approximately 0.4°C in
510 temperature is associated with a decrease of roughly 570 million US\$ in AVA
511 and 880 million US\$ in GDP.

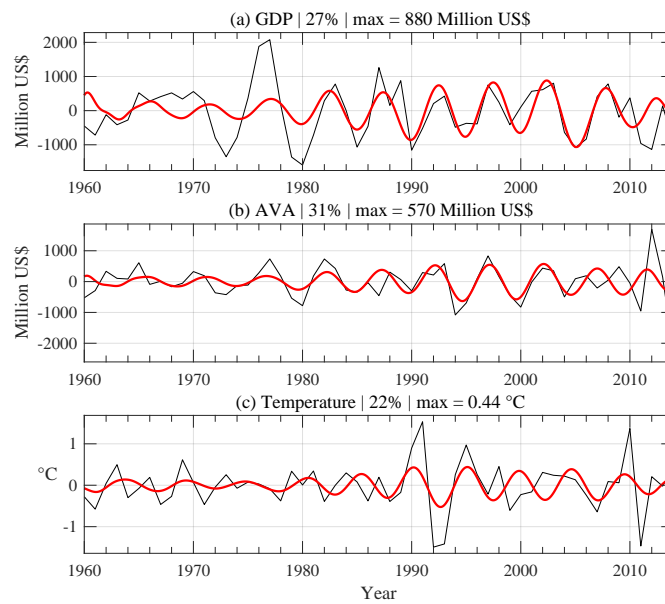


Figure 8: Trend residuals (light black) and reconstruction with the RCs (heavy red) corresponding to the coupled 5.0-year mode in Sudan; for (a) GDP, (b) AVA, and (c) temperature. M-SSA and MC test parameter values equal those in Fig. 4, except that an additional EOF pair, with a period of 3.6 years, is now excluded from the composite null hypothesis as well; see parentheses in Table 2.

512 The absence of any coupled climate-economic modes involving rainfall, though,
513 does not necessarily mean that rainfall has no effect on Sudan’s agriculture at all.
514 We have focused here on interannual variability with 2–10-year periods, while
515 agriculture in Sudan could be influenced by longer-term variations in rainfall,
516 which are captured by the lowest-frequency EOFs. These low-frequency EOFs,
517 though, have been excluded from the composite null hypothesis.

518 *6.3. A pervasive quasi-biennial mode in Burkina Faso*

519 In Burkina Faso, the M-SSA analysis finds a quasi-biennial 2.4-year mode
520 to be significant in all four indicators, cf. again Table 2. The corresponding
521 RCs are shown in Fig. 9. In AVA, this mode provides a good fit to the trend
522 residuals and it captures 18% of the residuals’ variance. In GDP, however, this
523 mode plays only a minor role and captures no more than 3% of the variance.
524 The RCs in the two climate indicators are anti-correlated, with higher rainfall
525 levels and lower temperatures having a positive effect on the economy.

526 The amplitude ratio of the RCs suggests that an approximate 2 mm/year
527 increase in rainfall and 0.2°C decrease in temperature correspond to an increase
528 of roughly 110 million US\$ in AVA, but only about 50 million US\$ in GDP.
529 This finding shows that Burkina Faso is less sensitive to rainfall variations in
530 the 2.4-year coupled mode than Niger is in its 4.1-year mode, cf. Fig 7. Such a
531 lesser sensitivity could be, once more, a result of Burkina Faso’s being closer to
532 the core of the rainbelt, so that year-to-year shifts are less critical for Burkina
533 Faso than for Niger. Lastly, the higher value obtained in AVA compared to
534 GDP is consistent with the greater volatility of agriculture observed in section
535 4.2.

536 **7. Discussion**

537 In the present study, we applied the advanced spectral M-SSA method to
538 study the influence of climate variability on the economy, in particular the
539 agricultural sector. Our dataset covers several economies in the Sahel region in

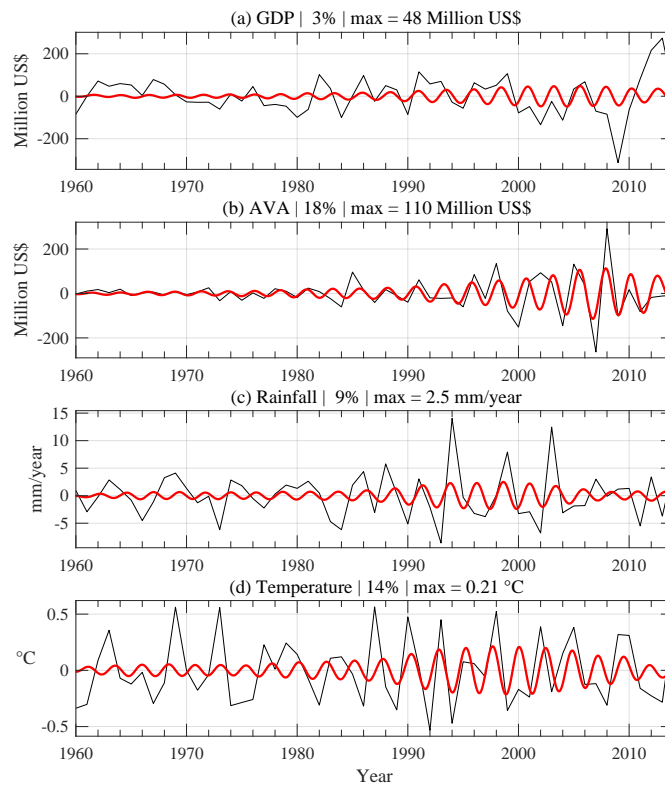


Figure 9: Trend residuals (light black) and reconstruction with the RCs (heavy red) corresponding to the coupled 2.4-year mode in Burkina Faso; for (a) GDP, (b) AVA, (c) rainfall, and (d) temperature. M-SSA and MC test parameters as in Fig. 4, except that three other EOF pairs, with a period of 4.8 years, 2.8 years, and 2.2 years, are now excluded from the composite null hypothesis as well; see parentheses in Table 2.

540 which we are able to identify coupled climate-economic modes on interannual
541 time scales that have high statistical significance of 97.5%–99%.

542 [Berry and Okulicz-Kozaryn \(2008\)](#) used a higher-order AR model to look for
543 ENSO signals in the short-term fluctuations of the US economy. These authors,
544 however, were not able to identify any co-cyclicity between ENSO and US
545 macroeconomic indicators. Their negative result may be due to a number of
546 causes, such as the size and complexity of the US, in which locally important
547 climatic effects vanish; the fact that the agricultural sector accounts for as little
548 as 1% of the US GDP in 2015; or to the lesser ability of their methodology to
549 identify small but relatively regular effects in a sea of noisy fluctuations. On the
550 other hand, ENSO variability has been linked to agricultural fluctuations and
551 crop yields in Mexico ([Dilley, 1997](#)), Indonesia ([Naylor et al., 2001](#)), and China
552 ([Deng et al., 2010](#)).

553 In the case of the developing countries at hand, it seems that the important
554 share of the agricultural sector, along with a low development of modern agri-
555 cultural practices such as irrigation, enhances the sensitivity to climate signals
556 in the economy. In [Sec. 6](#), the AVA index was always involved in the cou-
557 pled climate-economic modes we found to have high statistical significance. For
558 Sudan and Burkina Faso, this climate signal was visible in GDP as well.

559 In the present study, we have focused on climate variability on interannual
560 time scales, with a period of 2–10 years. Although the Sahel region is often
561 considered as one entity, we found considerable diversity in both the Sahel’s
562 climate and economic system. It therefore happens that the coupled climate-
563 economic modes strongly differ from country to country in their characteristics,
564 even between neighboring countries.

565 We have seen, in particular, that ENSO’s quasi-biennial and quasi-quadrennial
566 oscillatory modes ([Rasmusson and Carpenter, 1982](#); [Jiang et al., 1995](#); [Ghil
567 et al., 2002](#)) had only very little influence on the region’s economies as a whole;
568 see again [Fig. 5\(c\)](#). For Burkina Faso, though, we did identify a persistent
569 2.4-year mode, which could be linked to this country’s geographical location
570 and to the well-known impact of ENSO on the West African monsoon ([Nichol-](#)

571 [son, 2013](#)). For the other countries, however, a direct link to ENSO could not
572 demonstrated by the present analysis, while large-scale climate phenomena on
573 longer time scales might still play a role ([Chang et al., 2015](#)).

574 Overall, the RCs of the coupled climate-economic modes have been shown to
575 provide a rather good reconstruction of the temporal evolution of the AVA trend
576 residuals. The number of distinct oscillatory modes in the climate, as well as
577 the economic system, does suggest, however, that studying climate impacts on
578 the region’s agriculture should eventually go beyond a simple linear regression.

579 While several climate modes were identified on interannual time scales, only
580 a few of them appear to be coupled to the Sahel’s economies. On the other hand,
581 a few purely economic modes were identified as well and raise the question of
582 endogenous economic dynamics and other factors outside the scope of this study.

583 In the present M-SSA analysis, we focused on the conceptually simplest
584 hypothesis of a one-to-one coupling with similar periods between the climate
585 and economic system. This restriction was chosen for the sake of simplicity, and
586 not because the methodology is limited to the analysis of linear systems alone.
587 Thus, for instance, [Groth and Ghil \(2011, 2017\)](#) found M-SSA helpful in the
588 synchronization analysis of coupled chaotic oscillators, both in the climate and
589 in the macroeconomics realm. Proceeding in this direction, though, will require
590 considerable work, especially given the shortness of the available datasets.

591 The coupling of the two systems through a few weak oscillatory modes is
592 interesting insofar as it is consistent with theoretical predictions about weakly
593 coupled chaotic systems (e.g., [Boccaletti et al., 2002](#), and references therein). In
594 the latter, the complex behavior in each of the systems can lead to a complex
595 synchronization process, in which weaker oscillatory modes get synchronized
596 first ([Groth and Ghil, 2011](#)).

597 Finally, with respect to the assessment of climate impacts, the analysis pro-
598 vides some helpful insights into the sensitivity as well. The amplitude ratio in
599 the coupled modes between the rainfall RCs and the AVA ones, for instance,
600 provides a quantitative estimate of this sensitivity that is consistent with the
601 country’s exposure to rainfall variability. This ratio shows that Burkina Faso

602 and Senegal, both closer to the core of the rainbelt, are less susceptible to rain-
603 fall variations, while Niger's being closer to the rainbelt's northern edge makes
604 it more susceptible; see again Fig. 1. Although not capturing the complete, pos-
605 sibly nonlinear effects of rainfall on agriculture, the present analysis provides a
606 first-order approximation of the influence of year-to-year variations in rainfall
607 on the economy.

608 8. Summary

609 Since its introduction into the analysis of nonlinear and complex systems
610 (Broomhead and King, 1986a,b), M-SSA has found numerous applications in the
611 climate sciences (Ghil et al., 2002, and references therein). Recently, M-SSA has
612 also been applied to study macroeconomic activity and global synchronization
613 of business cycles (Groth et al., 2015; Sella et al., 2016; Groth and Ghil, 2017).

614 The present work goes a step further and applies the M-SSA methodology to
615 study coupled climate-economic behavior; it also provides a novel significance
616 test to assess whether signals of interannual climate variability can be identified
617 in regional economic behavior. We focused on the Sahel region, including the
618 six countries of Burkina Faso, Chad, Mauritania, Niger, Senegal, and Sudan, for
619 which economic, as well as climatic data were available since 1960; see Secs. 1–3.

620 The Sahel is characterized by large variations in rainfall levels that are due
621 to strong seasonality in the rainbelt position. The rainfall is generally limited
622 to the boreal summer months, while small year-to-year shifts in the rainbelt
623 position can have drastic consequences on the agricultural sector, cf. Sec. 4.

624 Although often considered as a single geographic entity, our results show
625 considerable diversity in the Sahel's climatic and economic dynamics. This
626 diversity is reflected in a number of significant oscillatory modes in each of the
627 two systems, cf. Sec. 5.

628 We have chosen, therefore, to study coupled climate-economic behavior in
629 each country individually, cf. Sec. 6. In the present analysis, we are able to
630 identify four coupled climate-economic modes with high statistical significance,

631 from 97.5% to 99%; see Table 2.

632 These four modes are present in Burkina Faso, Niger, Senegal and Sudan,
633 and capture the temporal evolution of the agricultural sector in these countries
634 quite well. In Chad and Mauritania, on the other hand, the present, rather
635 short dataset did not allow us to identify coupled climate-economic behavior.
636 The short dataset obliged us to limit ourselves to study interannual variability
637 with periods of 2–10 years, while longer-term climate variations ([Chang et al.,](#)
638 [2015](#)) could still play a role.

639 Despite the number of distinct climate modes we found to be statistically
640 significant in the Sahel region, it turned out that only a few of them manifest
641 themselves as coupled climate-economic modes. In Burkina Faso, we observe a
642 possible influence of ENSO’s quasi-biennial oscillatory mode, possibly because
643 of this country’s high exposure to the West African monsoon. For the other
644 countries, however, a direct link to ENSO is less clear from the present analysis,
645 while connections to other large-scale climatic phenomena have to be left for
646 future studies.

647 Finally, we have shown that the M-SSA analysis provides helpful insights
648 into the sensitivity analysis of the agricultural sector with respect to year-to-
649 year variations in rainfall, cf. Sec. 6. We showed, for example, that in Niger
650 the sensitivity to variations in annual rainfall levels is around three times higher
651 than in Burkina Faso and Senegal. This difference in sensitivity is likely to be
652 due to differences in the countries’ exposure to rainfall during the boreal summer
653 months.

654 The wealth and variety of the present results suggests the need for refin-
655 ing further the application of advanced spectral methods like M-SSA to study
656 the complex interactions between the climate and economic system. Doing so
657 should thus help answer N. Sterns call for better methods to help the world take
658 the road of a sounder future ([Stern, 2016](#)).

659

660 **Declaration of interest**

661 The authors have no competing interests to declare.

662 The present work was part of Vivien Sainte Fare Garnot's master thesis and
663 was carried out before he joined an energy analytics company.

664 **References**

665 Alessio, S.M., 2016. Digital Signal Processing and Spectral Analysis for Scien-
666 tists: Concepts and Applications. Springer.

667 Allen, M.R., Robertson, A.W., 1996. Distinguishing modulated oscillations from
668 coloured noise in multivariate datasets. *Climate Dynamics* 12, 775–784.

669 Allen, M.R., Smith, L.A., 1996. Monte Carlo SSA: Detecting irregular oscilla-
670 tions in the presence of colored noise. *Journal of Climate* 9, 3373–3404.

671 Becker, A., Finger, P., Meyer-Christoffer, A., Rudolf, B., Schamm, K., Schnei-
672 der, U., Ziese, M., 2013. A description of the global land-surface precipita-
673 tion data products of the global precipitation climatology centre with sample
674 applications including centennial (trend) analysis from 1901-present. *Earth*
675 *System Science Data* 5, 71.

676 Berry, B.J.L., Okulicz-Kozaryn, A., 2008. Are there ENSO signals in the
677 macroeconomy? *Ecological Economics* 64, 625–633.

678 Boccaletti, S., Kurths, J., Osipov, G., Valladares, D., Zhou, C., 2002. The
679 synchronization of chaotic systems. *Phys. Rep.* 366, 1–101.

680 Broomhead, D.S., King, G.P., 1986a. Extracting qualitative dynamics from
681 experimental data. *Physica D: Nonlinear Phenomena* 20, 217–236.

682 Broomhead, D.S., King, G.P., 1986b. On the qualitative analysis of experimental
683 dynamical systems, in: Sarkar, S. (Ed.), *Nonlinear Phenomena and Chaos*.
684 Adam Hilger, Bristol, England, pp. 113–144.

-
- 685 Burns, A.F., Mitchell, W.C., 1946. Measuring Business Cycles. National Bureau
686 of Economic Research, New York.
- 687 Chang, C.P., Ghil, M., Latif, M., Wallace, J.M. (Eds.), 2015. Climate Change:
688 Multidecadal and Beyond. World Scientific Publ. Co./Imperial College Press.
- 689 Chen, M., Xie, P., Janowiak, J.E., Arkin, P.A., 2002. Global land precipitation:
690 A 50-yr monthly analysis based on gauge observations. *Journal of Hydrometeo-*
691 *rology* 3, 249–266.
- 692 Cogley, T., Nason, J.M., 1995. Effects of the Hodrick-Prescott filter on trend
693 and difference stationary time series: Implications for business cycle research.
694 *Journal of Economic Dynamics and Control* 19, 253–278.
- 695 Deng, X., Huang, J., Qiao, F., Naylor, R.L., Falcon, W.P., Burke, M., Rozelle,
696 S., Battisti, D., 2010. Impacts of El Niño-Southern Oscillation events on
697 China’s rice production. *Journal of Geographical Sciences* 20, 3–16.
- 698 Dilley, M., 1997. Climatic factors affecting annual maize yields in the valley of
699 Oaxaca, Mexico. *International Journal of Climatology* 17, 1549–1557.
- 700 Feliks, Y., Groth, A., Robertson, A.W., Ghil, M., 2013. Oscillatory climate
701 modes in the Indian Monsoon, North Atlantic and Tropical Pacific. *Journal*
702 *of Climate* 26, 9528–9544.
- 703 Georganos, S., Abdi, A.M., Tenenbaum, D.E., Kalogirou, S., 2017. Examining
704 the NDVI-rainfall relationship in the semi-arid Sahel using geographically
705 weighted regression. *Journal of Arid Environments* 146, 64–74.
- 706 Ghil, M., Allen, M.R., Dettinger, M.D., Ide, K., Kondrashov, D., Mann, M.E.,
707 Robertson, A.W., Saunders, A., Tian, Y., Varadi, F., 2002. Advanced spectral
708 methods for climatic time series. *Reviews of Geophysics* 40.
- 709 Ghil, M., Vautard, R., 1991. Interdecadal oscillations and the warming trend
710 in global temperature time series. *Nature* 350, 324–327.

-
- 711 Groth, A., Ghil, M., 2011. Multivariate singular spectrum analysis and the road
712 to phase synchronization. *Physical Review E* 84, 036206.
- 713 Groth, A., Ghil, M., 2015. Monte Carlo singular spectrum analysis (SSA) revis-
714 ited: Detecting oscillator clusters in multivariate datasets. *Journal of Climate*
715 28, 7873–7893.
- 716 Groth, A., Ghil, M., 2017. Synchronization of world economic activity. *Chaos:*
717 *An Interdisciplinary Journal of Nonlinear Science* 27, 127002.
- 718 Groth, A., Ghil, M., Hallegatte, S., Dumas, P., 2015. The role of oscillatory
719 modes in U.S. business cycles. *OECD Journal of Business Cycle Measurement*
720 *and Analysis* 2015, 63–81.
- 721 Harvey, A.C., Jaeger, A., 1993. Detrending, stylized facts and the business
722 cycle. *Journal of Applied Econometrics* 8, 231–247.
- 723 Janicot, S., Moron, V., Fontaine, B., 1996. Sahel droughts and enso dynamics.
724 *Geophysical Research Letters* 23, 515–518.
- 725 Janowiak, J.E., 1988. An investigation of interannual rainfall variability in
726 africa. *Journal of Climate* 1, 240–255.
- 727 Jiang, N., Neelin, J.D., Ghil, M., 1995. Quasi-quadrennial and quasi-biennial
728 variability in the equatorial Pacific. *Climate Dynamics* 12, 101–112.
- 729 Karhunen, K., 1946. Zur Spektraltheorie stochastischer Prozesse. *Annales*
730 *Academiae Scientiarum Fennicae. Ser. A1, Math. Phys.* 34.
- 731 Kitchin, J., 1923. Cycles and trends in economic factors. *Review of Economics*
732 *and Statistics* 5, 10–16.
- 733 Loève, M., 1945. Fonctions aléatoires de second ordre. *Comptes Rendus de*
734 *l'Académie des Sciences Paris* 220, 380.
- 735 Masih, I., Maskey, S., Mussá, F., Trambauer, P., 2014. A review of droughts
736 on the African continent: a geospatial and long-term perspective. *Hydrology*
737 *and Earth System Sciences* 18, 3635.

-
- 738 Naylor, R.L., Falcon, W.P., Rochberg, D., Wada, N., 2001. Using El
739 Niño/Southern Oscillation climate data to predict rice production in Indone-
740 sia. *Climatic Change* 50, 255–265.
- 741 Nelson, C.R., Kang, H., 1981. Spurious periodicity in inappropriately detrended
742 time series. *Econometrica* 49, 741–751.
- 743 Nicholson, S.E., 2013. The West African Sahel: A review of recent studies on
744 the rainfall regime and its interannual variability. *ISRN Meteorology* 2013.
- 745 Portes, L.L., Aguirre, L.A., 2016. Matrix formulation and singular-value decom-
746 position algorithm for structured varimax rotation in multivariate singular
747 spectrum analysis. *Physical Review E* 93, 052216.
- 748 Rasmusson, E.M., Carpenter, T.H., 1982. Variations in tropical sea surface tem-
749 perature and surface wind fields associated with the Southern Oscillation/El
750 Niño. *Monthly Weather Review* 110, 354–384.
- 751 Rockström, J., Karlberg, L., et al., 2009. Zooming in on the global hotspots of
752 rainfed agriculture in water-constrained environments, in: Wani, S.P., Rock-
753 ström, J., Theib, O. (Eds.), *Rainfed Agriculture: Unlocking the Potential*.
754 CABI Wallingford, UK, pp. 36–43.
- 755 Sella, L., Vivaldo, G., Groth, A., Ghil, M., 2016. Economic cycles and their
756 synchronization: A comparison of cyclic modes in three European countries.
757 *Journal of Business Cycle Research* 12, 24–48.
- 758 Stern, N., 2016. Economics: Current climate models are grossly misleading.
759 *Nature* 530, 407–409.
- 760 Vautard, R., Ghil, M., 1989. Singular spectrum analysis in nonlinear dynamics,
761 with applications to paleoclimatic time series. *Physica D: Nonlinear Phenom-
762 ena* 35, 395–424.